Article no. 10

THE CIVIL ENGINEERING JOURNAL 1-2023

RESEARCH ON A SAFETY EVALUATION SYSTEM FOR RAILWAY-TUNNEL STRUCTURES BY FUZZY COMPREHENSIVE EVALUATION THEORY

Yanfeng Li[1], Jialong Li[1], Jihe Zhao[2], Tongfeng Zhao[3] and Dong Guo[4]

1. *Shenyang Jianzhu University, School of Transportation and Geomatics Engineering, Shenyang 110168, China; lyfneu@126.com, lijialong@stu.sjzu.edu.cn*
2. *Liaoning Technical University, School of Civil Engineering, Fuxin 123000, China; zjh321814@163.com*
3. *Liaoning Provincial College of Communications, Department of Road and Bridge Engineering, Shenyang 110122, China; 734849351@qq.com*
4. *Dalian Branch of China Railway Ninth Bureau Group Co., Ltd., Dalian 116019, China; 457992075@qq.com*

ABSTRACT

Long-term health detection of railway-tunnels is the development direction and trend of future railway tunnel research. Based on the actual engineering of a railway tunnel, this study developed a safety evaluation model for railway tunnel structures using a fuzzy comprehensive evaluation method and examined a health state evaluation method suitable for most railway tunnel structures. The results showed that the evaluation method comprehensively reflected the impact of various factors, which had strong practicality. The evaluation results were clear, accurate, and consistent with engineering practice. When using the safety factor index to study the stress of a railway tunnel structure, Midas/civil analysis showed that different levels of the surrounding rock structural vault in railway tunnels were in a tensile, control-bearing capacity state. When calculating safety factors, the range of a 60° central angle of a railway tunnel vault was calculated according to the tensile control-bearing capacity. Theoretical formulas of the range of the centre angle φ_0 of the vault tension zone were derived and then verified by experiments and numerical analysis.

KEYWORDS

Railway tunnels, Safety factor, Tensile range of vault, Safety evaluation, Fuzzy comprehensive evaluation

INTRODUCTION

With the rapid development of China's railway tunnel engineering and the continuous extension of construction, China has put forward higher requirements for the safety and maintenance of railway tunnels. To improve maintenance efficiency and quality, long-term structural health detection and evaluation must be performed. Therefore, an evaluation method based on the safety of railway tunnels was proposed here. The evaluation method, including monitoring and evaluating the structural health status of railway tunnels, was simulated by fuzzy comprehensive evaluation theory.

Relevant experts at home and abroad have begun to pay attention to the long-term structural health status of tunnels, establishing a long-term structural-safety detection system and formulating a corresponding regulatory system [1–3]. The system has achieved great results in terms of structural-health monitoring sensor technology and detection systems [4, 5]. Long-term monitoring of tunnels based on fiber detection technology using the Brillouin optical frequency domain (BOFDA) has been reported [6], and its technology used to analyse and study the factors of strain loss, which provides a theoretical basis for engineering practice. In the Asian Railway Tunnel Project, the risk assessment of tunnel safety is divided into four levels [7]. Based on structural destructive testing, non-destructive testing evaluations, static, and 3D nonlinear analysis, Muhammad F has proposed a proper structural health monitoring (SHM) system that will extend the life cycle of a bridge with minimal repair costs and reduced risk of failure [8]. Stanislaw W has proposed a method of structural monitoring using measurement of vertical displacements realized optically by horizontally directed laser beam [9]. Different evaluation methods for evaluating tunnels have been reported [10–13]. These methods have been applied to various types of tunnels, and their effectiveness and practicality of these methods verified. After consulting a large number of studies, the current safety assessment methods for railway tunnels have been found not unified and there is a lack of practical engineering cases and data on the health status of tunnel structures during operation and thus not convincing. Therefore, it is of great significance to establish a system of railway-tunnel structural safety evaluation indicators based on certain rationality, reliability, and practicality.

Using a railway tunnel, as the background, this study used research data, software testing, data analysis, and theoretical analytical methods. Specific research content, with potentially dangerous sources recognized as evaluation indicators, was used to combine on-site measurement information. The safety factor of a railway tunnel was analysed and determined by Midas/civil analysis. Then, different levels of surrounding rock structure of the railway tunnel vault stress state were analysed and theoretical formulas of the range of the centre angle $\varphi 0$ of the vault tension zone derived and their accuracy verified. Finally, the safety of the railway tunnel was evaluated using a fuzzy comprehensive evaluation method. According to the corresponding safety assessment standards, the final safety level of the actual project of the railway tunnel was obtained. Thus, a system of railway-tunnel structural safety assessment indicators with certain rationality, reliability, and practicality was established.

THEORETICAL STUDY OF THE TENSILE CONTROL RANGE OF RAILWAY TUNNEL STRUCTURES

Railway tunnel engineering background

The engineering background of this research was as follows: the mileage of the railway tunnel was DK34+275 to DK42+895, with a total length of 8620 m, longitudinal slope of 6.0‰, and maximum depth of 398 m. The entrance to this tunnel was flat, the slope ~20o, and intersection angle with the contour line at ~80°. The exit position of this tunnel was flat land, slope ~10°, and intersection angle between the hole and contour lines at 70–80°. According to geological surveys and drilling, the railway tunnel stratum was described as gravel soil, granite, strongly weathered rock, and weakly weathered rock, from new to old, respectively. The depth of water level was 0.5–21.7 m and the permeability coefficient of the stratum recommended as K = 0.00877–0.0698 m/d. The initial support included rock bolts, steel mesh, shotcrete, and steel frame. The secondary lining was divided into 4 types of surrounding rock. The concrete grades of the secondary lining were C30 and C35 and the thickness 30–45 cm.

The calculation of the railway tunnel structure adopted the “load-structure” model [14], and the safety factors calculated by the allowable stress method [15]. According to the Midas/civil finite element simulation, the bending moments and axial forces of surrounding rock at all grades of the railway tunnel were obtained. Simulation research has indicated that the safety of the tunnel is mainly affected by axial forces. Calculating the safety factors of the vault, arch waist, and inverted arch of the surrounding rock at all levels of the railway tunnel, analysis showed that the axial force eccentricities e0 of the vault of the surrounding rock of levels II, IV, and V of the railway tunnel were greater than 0.2 h (h is the thickness of the section) and the vault controlled by tensile strength.

The establishment and analysis of the numerical model

The shaft digging method has a large laneway length, such that it can be transformed into a plane problem. The 1-m length of a longitudinal cross-section was calculated by the finite element method of a plane bar system. When the secondary lining was calculated, the carrying capacity of the initial support was not considered. The calculation diagram is shown in Figure 1.

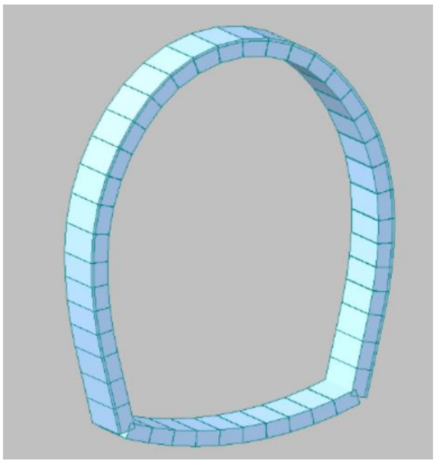

Fig. 1 – Finite element model design drawing

Lining defects mainly occurred in the granite area, with the mechanical parameters of different levels of surrounding rocks stipulated in the *Code for Design of Railway Tunnel TB10003-2016*; the reference values of these mechanical parameters are shown in Table 1. Referring to the geological prospecting of engineering field, the surrounding rock physical mechanical indicators were selected in Table 2, which contained the lining and other materials. For the elastic modulus of the surrounding rock, the deformation modulus was used as an elastic modulus to participate in calculation analysis. The main reason for this was that the deformation modulus, reflecting the stress and strain values of soil under local side limits, was obtained by *in situ* testing, which was applicable.

Tab.1 - Physical and mechanical indices of surrounding rock at all levels

Level	Volume weight γ (kN/m^3)	Elastic reaction coefficient *K* (MPa/m)	Deformation modulus *E* (GPa)	Poisson's ratio *v*	Frictional angle *φ* (°)	Cohesion *c* (MPa)	Calculation of friction angle φ_c (°)
Ⅱ	25–27	1200–1800	20–33	0.2–0.25	50–60	1.5–2.1	70–78
Ⅲ	23–25	500–1200	6–20	0.25–0.3	39–50	0.7–1.5	60–70
Ⅳ	20–23	200–500	1.3–6	0.3–0.35	27–39	0.2–0.7	50–60
Ⅴ	17–20	100–200	1–2	0.35–0.45	20–27	0.05–0.2	40–50
Ⅵ	15–17	<100	<1	1–2	<22	<0.1	30–40

Note: Loess and special surrounding rocks not included in the data and φ_c selected to calculate instead of *φ* and *c*.

Article no. 10

THE CIVIL ENGINEERING JOURNAL 1-2023

Tab. 2 - Selection of basic parameters of materials

Material	Volume weight (kN/m³)	Elastic modulus (MPa)	Poisson's ratio
Initial support	23	2.6e4	0.2
Secondary lining	25	3.15e4 (C35) 2.7e4 (C30)	0.2
Anchor	78	21e4	0.3

Note: Elastic modulus of soil is deformation modulus in numerical analysis software.

Formula derivation of the tensile control range of railway tunnel structures

In practical engineering, most tunnel metrics are calculated as symmetrical hinge less arches, whose two arch toes are equivalent to height. In this study, the tensile control range of tunnel structures were studied by referring to the calculation principle of elastic centre method and polar coordinate system method [16, 17]. The basic thoughts were as follows: The foundation structure with symmetric properties was used as the research object, whose load was divided into symmetric and anti-symmetric loads and the corresponding multi-unknown force simultaneous equations established. By adding a rigid arm, the vice coefficient (δ_{21} and δ_{12}) in the force method equation was 0, such that the problem of the simultaneous equation was transformed into several independent equation-solving problems. Superfluous unknown forces, X_1, X_2, and X_3, were set in the main direction, forming the basic structure of the force method of two extension beams. Among them, unknown forces, as in X_1, X_2, and X_3, were axial, bending moment, and shear forces, respectively (Figures 2 and 3).

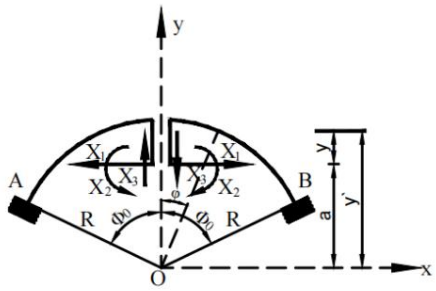

Fig. 2 – Symmetrical equal section without foot arch

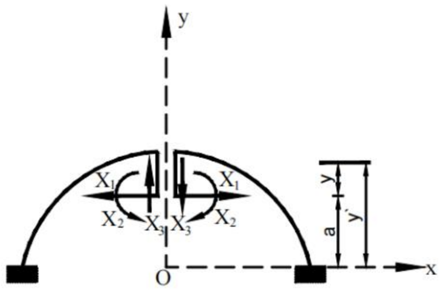

Fig. 3 – Basic structure of elastic centre method

Arched toe A and B are at the same height and the symmetry axis of the circular arch called the *y*-axis. The angle between one arched toe and *y*-axis was recorded as φ , which was represented by the arc. The radius of the scheme arch was *R*.

The following three basic equations of independent force were used to determine the multiple unknown forces, X_1, X_2, and X_3. In the following formula, δ_{11}、 δ_{12} are shape constants and Δ_{1P}、 Δ_{2P}、 Δ_{3P} are load constants, expressed as

$$\delta_{11}X_1 + \delta_{12}X_2 + \Delta_{1P} = 0,\ \delta_{21}X_1 + \delta_{22}X_2 + \Delta_{2P} = 0,\ \delta_{33}X_3 + \Delta_{3P} = 0 \tag{1}$$

A rigid arm was added to the vault and cut off at the symmetric axis position. In the two symmetric internal forces, X_1 and X_2, when the length of the vertical rigid arm changed, δ_{21}=δ_{12}=0. The following formula was thus obtained, expressed as

DOI 10.14311/CEJ.2023.01.0010

$$\delta_{11}X_1+\Delta_{1P}=0,\ \delta_{22}X_2+\Delta_{2P}=0,\ \delta_{33}X_3+\Delta_{3P}=0 \tag{2}$$

On the geometric symmetry axis *y* of the circular arch, the distance between the elastic centre and arc centre *O* was *a*, expressed as

$$a=\frac{\int y' \frac{1}{EI}ds}{\int \frac{1}{EI}ds}=\frac{R\sin\varphi_0}{\varphi_0} \tag{3}$$

where y' is the height between centroid of any cross-section and arc centre in the arch ring and φ_0 the angle from arch foot section to vault section.

The shape constants δ_{11}, δ_{22}, and δ_{33}, were only related to the geometric size of the arch, while the load constants, Δ_{1P}, Δ_{2P}, and Δ_{3P}, were related to the external load. Using the superposition principle, the final internal force expression of any section of arch ring was obtained as

$$M=\overline{M_1}X_1+\overline{M_2}X_2+\overline{M_3}X_3+M_P,\ Q=\overline{Q_1}X_1+\overline{Q_2}X_2+\overline{Q_3}X_3+Q_P,\ N=\overline{N_1}X_1+\overline{N_2}X_2+\overline{N_3}X_3+N_P \tag{4}$$

where $\overline{M_i}$, $\overline{Q_i}$, and $\overline{N_i}$ are the bending moment, shear force, and axial force, respectively, of any section of the basic structure under a unit unknown force X_i = 1 (*i* = 1,2,3), M_P, Q_P, and N_P are the bending moment, shear force, and axial force, respectively, of any section of the basic structure under any kind of external load, and *P* in M_P、Q_P、N_P indicate the load [18].

Under the action of a unit unknown force X_i = 1, the calculation formula of the internal force $\overline{M_i}$ and $\overline{N_i}$ of any section of basic structure is shown below.

When X_1 = 1 acts, $-\varphi_0 \le \varphi \le \varphi_0$, yielding Eq. (5) as

$$\overline{M_1}=1,\overline{N_1}=0 \tag{5}$$

When X_2 = 1acts, $-\varphi_0 \le \varphi \le \varphi_0$, yielding Eq. (6) as

$$\overline{M_2}=R\left(\frac{\sin\varphi}{\varphi}-\cos\varphi\right),\overline{N_2}=\cos\varphi \tag{6}$$

When X_3 = 1 acts, $-\varphi_0 \le \varphi \le \varphi_0$, yielding Eq. (7) as

$$\overline{M_3}=-R\sin\varphi,\overline{N_3}=\sin\varphi \tag{7}$$

The shape constants δ_{11}, δ_{22}, and δ_{33} were calculated only considering the influence of bending moment as an example and the shape constants under axial force and shear also calculated. The shape constants were calculated as:

$$\delta_{11}=\int\frac{\overline{M_1}^2}{EI}ds=\frac{1}{EI}\times2\int_0^{\varphi_0}\overline{M_1}^2Rd\varphi=\frac{2\varphi_0R}{EI}$$
$$\delta_{22}=\int\frac{\overline{M_2}^2}{EI}ds=\frac{1}{EI}\times2\int_0^{\varphi_0}\overline{M_2}^2Rd\varphi=\frac{R^3}{EI}\left(\varphi_0+\sin\varphi_0\cos\varphi_0-\frac{2\sin^2\varphi_0}{\varphi_0}\right) \quad (8)$$
$$\delta_{33}=\int\frac{\overline{M_3}^2}{EI}ds=\frac{1}{EI}\times2\int_0^{\varphi_0}\overline{M_3}^2Rd\varphi=\frac{R^3}{EI}\left(\varphi_0-\sin\varphi_0\cos\varphi_0\right)$$

where E is the elastic modulus of arch ring material, I the inertial moment of arch cross-section, and A the cross-sectional area.

The internal force, M_P and N_P, and load constants, Δ_{1P}, Δ_{2P}, and Δ_{3P}, of any section of the basic structure under different external loads were calculated by the following formula,

$$\Delta_{ip}=\frac{1}{EI}\int_s\overline{M_i}M_Pds(i=1,2,3),\Delta_{ip}=\frac{1}{EI}\int_s\overline{N_i}N_Pds(i=1,2,3) \quad (9)$$

According to the actual railway tunnel project and the following two kinds of external load forms, the calculation formulas of internal force, M_P and N_P, and load constants, Δ_{1P}, Δ_{2P}, and Δ_{3P}, of any section of the basic structure under different loads were deduced.

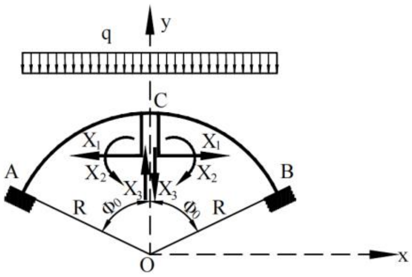

Fig. 4 – Arch span subjected to vertical uniform load q

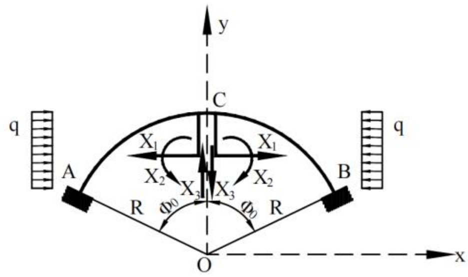

Fig. 5 – Arch span under action of horizontal distributed load q

(1) When the arch span was subjected to vertical uniform load q (Figure 4):

The calculation formula of internal forces, M_P and N_P, of an arbitrary section in the basic structure was

$$\begin{cases}M_P=-\frac{1}{2}qR^2\sin^2\varphi \\ N_P=qR\sin^2\varphi\end{cases}(0\le\varphi\le\varphi_0) \quad (10)$$

The calculation formula of load constants Δ_{1P}, Δ_{2P}, and Δ_{3P} was

$$\Delta_{1P}=\frac{1}{EI}\int_0^{\varphi_0}\overline{M_1}M_Pd\varphi=\frac{qR^3}{EI}\left[\frac{1}{4}\left(\sin\varphi_0\cos\varphi_0-\varphi_0\right)\right]$$
$$\Delta_{2P}=\frac{1}{EI}\int_0^{\varphi_0}\overline{M_2}M_Pd\varphi=\frac{qR^4}{EI}\left\{\frac{\sin\varphi_0}{\varphi_0}\left[\frac{1}{4}\left(\sin\varphi_0\cos\varphi_0-\varphi_0\right)\right]+\frac{1}{6}\sin^3\varphi_0\right\} \quad (11)$$
$$\Delta_{3P}=\frac{1}{EI}\int_0^{\varphi_0}\overline{M_3}M_Pd\varphi=\frac{qR^4}{EI}\left[\frac{1}{6}\left(\cos^3\varphi_0-3\cos\varphi_0+2\right)\right]$$

(2) When the arch span was subjected to a horizontal uniform load q (Figure 5):

The calculation formula of internal forces, M_P and N_P, of the arbitrary section in the basic structure was:

$$\begin{cases} M_P = \frac{1}{2}qR^2\left(2\cos\varphi - 1 - \cos^2\varphi\right) \\ N_P = qR\left(\cos\varphi - 1\right) \end{cases} (0 \le \varphi \le \varphi_0) \tag{12}$$

The calculation formula of load constant Δ_{1P}, Δ_{2P}, and Δ_{3P} was:

$$\begin{aligned} \Delta_{1P} &= \frac{1}{EI}\int_0^{\varphi_0}\overline{M_1}M_P d\varphi = \frac{qR^3}{EI}\left(\sin\varphi_0 - \frac{1}{8}\sin 2\varphi_0 - \frac{3}{4}\varphi_0\right) \\ \Delta_{2P} &= \frac{1}{EI}\int_0^{\varphi_0}\overline{M_2}M_P d\varphi = \frac{qR^4}{2EI}\left[\frac{\sin\varphi_0}{\varphi_0}\left(2\sin\varphi_0 - \frac{1}{4}\sin\varphi_0 - \frac{3}{2}\varphi_0\right) - \left(\varphi_0 + \sin\varphi_0\cos\varphi_0 - 2\sin\varphi_0 + \frac{1}{3}\sin^3\varphi_0\right)\right] \\ \Delta_{3P} &= \frac{1}{EI}\int_0^{\varphi_0}\overline{M_3}M_P d\varphi = \frac{qR^4}{2EI}\left(\sin^2\varphi_0 + \cos\varphi_0 + \frac{1}{3}\cos^3\varphi_0 - \frac{4}{3}\right) \end{aligned} \tag{13}$$

The axial force of any section of the arch ring was calculated to be $N = \overline{N_1}X_1 + \overline{N_2}X_2 + \overline{N_3}X_3 + N_P$, where $X_1 = -\frac{\Delta_{1P}}{\delta_{11}}$、$X_2 = -\frac{\Delta_{2P}}{\delta_{22}}$、$X_3 = -\frac{\Delta_{3P}}{\delta_{33}}$.

When the arch span was subjected to a vertical uniform load q, the result was:

$$\begin{aligned} X_1 &= -\frac{\Delta_{1P}}{\delta_{11}} = -\frac{qR^2\left[\frac{1}{4}\left(\sin\varphi_0\cos\varphi_0 - \varphi_0\right)\right]}{2\varphi_0} \\ X_2 &= -\frac{\Delta_{2P}}{\delta_{22}} = -\frac{qR\left\{\frac{\sin\varphi_0}{\varphi_0}\left[\frac{1}{4}\left(\sin\varphi_0\cos\varphi_0 - \varphi_0\right)\right] + \frac{1}{6}\sin^3\varphi_0\right\}}{\left(\varphi_0 + \sin\varphi_0\cos\varphi_0 - \frac{2\sin^2\varphi_0}{\varphi_0}\right)} \\ X_3 &= -\frac{\Delta_{3P}}{\delta_{33}} = -\frac{qR\left[\frac{1}{6}\left(\cos^3\varphi_0 - 3\cos\varphi_0 + 2\right)\right]}{\varphi_0 - \sin\varphi_0\cos\varphi_0} \end{aligned} \tag{14}$$

When the arch span was subjected to horizontal uniform load q, the result was:

$$\begin{aligned} X_1 &= -\frac{\Delta_{1P}}{\delta_{11}} = -\frac{qR^2\left(\sin\varphi_0 - \frac{1}{8}\sin 2\varphi_0 - \frac{3}{4}\varphi_0\right)}{2\varphi_0} \\ X_2 &= -\frac{\Delta_{2P}}{\delta_{22}} = -\frac{qR\left[\frac{\sin\varphi_0}{\varphi_0}\left(2\sin\varphi_0 - \frac{1}{4}\sin 2\varphi_0 - \frac{3}{2}\varphi_0\right) - \left(\varphi_0 + \sin\varphi_0\cos\varphi_0 - 2\sin\varphi_0 + \frac{1}{3}\sin^3\varphi_0\right)\right]}{2\left(\varphi_0 + \sin\varphi_0\cos\varphi_0 - \frac{2\sin^2\varphi_0}{\varphi_0}\right)} \\ X_3 &= -\frac{\Delta_{3P}}{\delta_{33}} = -\frac{qR\left(\sin^2\varphi_0 + \cos\varphi_0 + \frac{1}{3}\cos^3\varphi_0 - \frac{4}{3}\right)}{2(\varphi_0 - \sin\varphi_0\cos\varphi_0)} \end{aligned} \tag{15}$$

Using the exchange decree sinφ_0 = x and cosφ_0 = y, the axial force of any section of the arch ring was obtained as:

$$N = y\left\{\frac{-\frac{qR^4}{EI}\left[\frac{x}{\varphi_0}\left(\frac{1}{4}xy-\varphi_0\right)+\frac{1}{6}x^3\right]}{\frac{R^3}{EI}\left(\varphi_0+xy-\frac{2x^2}{\varphi_0}\right)}\right\}+x\left\{\frac{-\frac{qR^4}{EI}\left[\frac{1}{6}\left(y^3-3y+2\right)\right]}{\frac{R^3}{EI}\left(\varphi_0-xy\right)}\right\}+qRx^2+qRy\left(y-1\right)$$
$$+y\left\{\frac{-\frac{qR^4}{2EI}\left[\frac{x}{\varphi_0}\left(2x-\frac{1}{2}xy-\frac{2}{3}\varphi_0\right)-\left(\varphi_0+xy-2x+\frac{1}{3}x^3\right)\right]}{\frac{R^3}{EI}\left(\varphi_0+xy-\frac{2x^2}{\varphi_0}\right)}\right\}+\sin\varphi_0\left\{\frac{-\frac{qR^4}{2EI}\left[x^2+y+\frac{1}{3}y^3-\frac{4}{3}\right]}{\frac{R^3}{EI}\left(\varphi_0-xy\right)}\right\} \tag{16}$$

After simplification, the unary cubic equation about x was obtained as:

$$12\left(\frac{N}{qR}-x^2-y^2\right)\varphi_0^3+\left(12x-6xy^2-12x^3-18xy+2x^3y\right)\varphi_0^2+(21x^2y^2+10x^4y^2-12x^4y$$
$$+18xy^2-19x^2y^3+12x^2y^4+12x^4-36\frac{N}{qR}x^2y^2-36\frac{N}{qR}x^2)\varphi_0+24\frac{N}{qR}x^3y-24x^5y$$
$$-24x^3y^3+24x^5+12x^3y-24x^3=0 \tag{17}$$

Verification and analysis of tensile control range of tunnel structure

Safety factors of concrete structure are stipulated in Chapter 8.5.2 of the *Code for Design of Railway Tunnel TB10003-2016*. Safety factors of concrete and masonry structures under main load are shown in Table 3. The minimum safety factor was 2.4 under ultimate compressive strength and the minimum safety factor 3.6 under ultimate tensile strength.

Tab. 3 - Strength safety factors of concrete and masonry structures

Material		Concrete		Masonry	
Load combination		Main load	Main load and additional load	Main load	Main load and additional load
Damage reason	Concrete or masonry reach ultimate compressive strength	2.4	2.0	2.7	2.3
	Concrete reaches ultimate tensile strength	3.6	3.0	—	—

When the axial eccentricity $e_0 = 0.2h$, the critical state of section tensile and compressive control bearing capacity was present. The safety factor K was 3.6 when the concrete reached its ultimate tensile strength, which was used as the basis for axial force calculations. Therefore, the range of tensile control bearing capacity of a railway tunnel was obtained, which had certain convenience for safety judgment of a railway tunnel and simplified its calculation. Taking the actual railway tunnel as an example, the specific parameters for verification of surrounding rock at all levels are shown in Table 4.

Tab. 4 - Calculation parameters of different level surrounding rock in the railway tunnel

Calculation parameters / Surrounding rock level	Tensile ultimate strength R_1 (kN/m³)	Thickness h (m)	Width b (m)	Axial force N (kN)	Radius R (m)	Vertical uniform load	Horizontal uniform load
II surrounding rock	2200	0.3	1	1604.2	2.8	27.0972	0
Ⅲ surrounding rock	2200	0.3	1	1604.2	2.8	50.0256	7.50384
Ⅳ surrounding rock	2400	0.35	1	1871.53	2.85	91.1772	20.5149
Ⅴ surrounding rock	2400	0.4	1	3500	2.9	160.9056	64.3622

According to equation derivations, specific parameters were introduced into the derivation for calculation and the angle of the tensile centre of the railway tunnel vault obtained. The specific results were as follows. The calculated central angle φ_0 of the tensile control bearing capacity was 34.9, 45.1, 38.7, and 30.3° for levels II, III, IV, and V of the surrounding rock, respectively. The vault section of the actual railway tunnel in levels II, IV, and V of the surrounding rock was tensile-controlled bearing capacity. When calculating the safety factor of the tunnel, the safety factor was calculated according to the tensile-controlled bearing capacity of the vault in the range of a 60° central angle of the railway tunnel section.

STUDY ON FUZZY COMPREHENSIVE EVALUATION THEORY OF THE RAILWAY TUNNEL

Fuzzy comprehensive evaluation theory

The safety of tunnel structure is affected by stress characteristics, geological conditions, structural defects and other factors. Therefore, in the process of safety assessment of tunnel structure, the influence of various factors must be fully considered, and its own characteristics must be considered. Using qualitative or quantitative evaluation methods alone cannot obtain accurate evaluation results.

Fuzzy comprehensive evaluation is a combination of qualitative and quantitative evaluation method. It can consider multiple factors and multiple types, and organically combine the fuzzy characteristics and diversity characteristics of influencing factors. The results are accurate and systematic. It is a more suitable evaluation method for engineering practice.

Fuzzy comprehensive evaluation is an analysis method based on fuzzy mathematics and is widely used in tunnel engineering. Multistage fuzzy comprehensive evaluation was based on fuzzy comprehensive evaluation and a basic model of vague comprehensive evaluation established, which reflected the status and functions of various evaluation factors in overall evaluation. Each influencing factor was analysed comprehensively and impact factors classified by levels. Initially, a first-level comprehensive evaluation was carried out and the evaluation results then used as evaluation indices for conducting a secondary comprehensive evaluation.

Fuzzy comprehensive evaluation theory is a comprehensive evaluation method considering multi-factor fuzzy mathematics [19]. The choice of these factors directly affected result evaluation. To ensure the accuracy, objectivity, and practicability of the evaluation results, the basic principles of systematics and universality must be followed when selecting the influencing factors for evaluation. The evaluation was based on considered factors, such as the geological environment of the railway tunnel, structural defects, and structural stress. The safety evaluation indicators of railway tunnels were set as:

(1) Engineering geological conditions N_1: rock quality index n_{11}, leakage water n_{12}, completeness of surrounding rock n_{13}, fault fracture zone n_{14}, rock characteristics of surrounding rock n_{15}, and *in situ* stress coefficient n_{16}.

(2) Structural defect N_2: lining thickness defect position n_{21}, effective thickness ratio of lining n_{22}, concrete strength n_{23}, and defect site of lining steel bar n_{24}.

(3) Structural stress N_3: lining pressure control n_{21} and lining tension control n_{22}.

(4) Other factors N_4: construction design level n_{11}, seismic fortification intensity n_{12}, and year of service n_{13}.

Determination of algorithm theoretical weight and membership function

A judgment matrix containing various indicators was established. Experts have considered the relative importance levels of each indicator and provided corresponding scores in accordance with a 1–9 scale method [20]. With this scale, 1 means that both are equally important, 3 that the former is slightly more important than the latter, 5 the former is significantly more important than the latter, 7 the former is strongly more important than the latter, and 9 the former is extremely more important than the latter. Thus, 2, 4, 6, and 8 means the importance is between two numbers. The analytic hierarchy process (AHP) [21] was used to determine the weight of railway tunnel structural safety factors. Then, the weight of each index was obtained by normalizing the corresponding feature vector. For a judgment matrix, a consistency test is often carried out to verify whether it is consistent with reality. On this basis, the consistency test of the obtained weights was carried out to ensure reliability of the subsequent sorting and decision-making. Professor Saaty [22] has believed that, if there is no big deviation between the obtained decision matrix and the consistency requirement, the decision matrix reaches “satisfactory consistency,” which was calculated here according to the definition of consistency index, expressed as:

$$CI = \frac{\lambda_{\max} - n}{n-1} \tag{18}$$

$$CR = \frac{CI}{RI} \tag{19}$$

where *CI* is the consistency index, *CR* the consistency ratio, *RI* the random consistency index, and *n* the order of the judgment matrix.

The consistency index *CI* was calculated using the maximum characteristic root $\lambda_{\max}$ of the judgment matrix and the consistency ratio calculated by the average random consistency index *RI*. When *CR* was <0.1, the decision matrix met the condition of "satisfactory consistency." When *CR* was >0.1, the decision matrix needed to be adjusted accordingly. The weights of various indicators of railway tunnel engineering are shown in Table 5.

Tab. 5 - Index Weight of a Railway Tunnel

Criterion layer	Weight	Index layer	Weight
Engineering geological conditions N_1	0.086036	Rock quality index n_{11}	0.1468
		Leakage water n_{12}	0.0811
		Completeness of surrounding rock n_{13}	0.0811
		Fault fracture zone n_{14}	0.2671
		Strength characteristics of surrounding rock n_{15}	0.1468
		In situ stress coefficient n_{16}	0.2671
Structural defect N_2	0.23945	Lining thickness defect position n_{21}	0.17697
		Effective thickness ratio of lining n_{22}	0.56649
		Concrete strength n_{23}	0.07099
		Defect site of lining steel bar n_{24}	0.18554
Structural stress N_3	0.521513	Lining pressure control n_{31}	0.8333
		Lining tension control n_{32}	0.1667
Other factors N_4	0.152997	Construction design level n_{41}	0.2000
		Seismic fortification intensity n_{42}	0.4000
		Year of service n_{43}	0.4000

The membership function was a means for obtaining the membership degree, which considers the operability of the project in engineering practice as well as objectivity. As the evaluation of each influencing factor had both quantitative and qualitative characteristics, the membership functions constructed should be different. Determining the membership function of four qualitative factors includes leakage water, integrity of surrounding rock, fault, and fracture zone. In defect location of lining thickness and lining reinforcement as well as construction design level, each index requires quantification. The evaluation interval of each factor can be divided into four levels: excellent (0.9), good (0.7), medium (0.5), and poor (0.3) [23]. The membership function was expressed by a trapezoidal function:

$$A(x)=\begin{cases}1 & x<a\\ \dfrac{b-x}{b-a} & a\leqslant x\leqslant b\\ 0 & b<x\end{cases}\qquad A(x)=\begin{cases}0 & x<a\\ \dfrac{x-a}{b-a} & a\leqslant x\leqslant b\\ 1 & b<x\end{cases}\qquad A(x)=\begin{cases}\dfrac{x-a}{b-a} & a\leqslant x<b\\ 1 & b\leqslant x<c\\ \dfrac{d-x}{d-c} & c\leqslant x\leqslant d\\ 0 & x<a or d<x\end{cases}\tag{20}$$

Smaller type　　Larger type　　Intermediate type

Miscellaneous factors and the axial force and bending moment of the main structure under load were expressed by a Gaussian distribution function, being:

$$A(x)=\begin{cases}1 & x\leqslant a\\ e^{-\left(\frac{x-a}{\sigma}\right)^2} & a<x\end{cases}\qquad A(x)=\begin{cases}0 & x\leqslant a\\ 1-e^{-\left(\frac{x-a}{\sigma}\right)^2} & a<x\end{cases}\qquad A(x)=e^{-\left(\frac{x-a}{\sigma}\right)^2}\ -\infty<x<+\infty a\tag{21}$$

Smaller type　　Larger type　　Intermediate type where $\sigma = \frac{x_{i+1} - x_i}{2\sqrt{-\ln 0.5}}$ is the average value of the interval of each factor at the security level and σ the corresponding variance.

FUZZY COMPREHENSIVE EVALUATION OF RAILWAY TUNNEL STRUCTURAL SAFETY

Based on the theory of fuzzy comprehensive evaluation, a safety evaluation model of the railway-tunnel structure was built. Fifteen factors affecting the safety of a tunnel structure in 4 categories were analyzed in detail. According to references [24, 25], the division standards of all influencing factors were standardized. Through the analysis of relevant literature and norms at home and abroad, it has been found that the assessment level should not be too high and the application of 4 levels of division has been widely applied, with level I a safe structure, level II a basic security structure, level III a great hidden-danger structure, and level IV an unstable structure.

This article focused on explaining the stress characteristics of railway tunnels. The second lining of railway tunnels is mainly affected by axial forces and bending moments. They are long-term engineering quality monitoring projects and are related to tunnel structural safety. According to a study regarding the tensile control angle range of railway tunnels, the safety factor level of the lining structure can be divided into tension and compression zones. Among these, safety level I means that the secondary lining of the tunnel bears a relatively small load and the safety factor of the bending moment and axial load higher by 2-fold than that specified in the specification. Basic safety level II means that the secondary lining bears a relatively large load, resulting in tiny cracks, with the safety factor at 1 to 2-fold that specified by the standard. The potential unsafe level III means that the tunnel lining structure has cracked or fallen off, but it can still bear the local load, such that the safety factor is less than the specified requirements but greater than 1. The unsafe level IV means that the tunnel lining having perforations and cracks, in which the load can no longer be carried and the safety factor <1.

In view of the universality of the evaluation system, level III surrounding rock of the actual railway tunnel project was selected to represent for safety evaluation. The detection of the railway tunnel is shown in Table 6.

Tab. 6: Detection of level III surrounding rock in the railway tunnel

Fuzzy comprehensive evaluation factors of tunnel safety		Detection
Engineering geological conditions	Rock quality index	Rock granite, rock mass relatively complete
	Leakage water	No water leakage, seasonal dripping on arch
	Completeness of surrounding rock	No voids exist in surrounding rock
	Fault fracture zone	No faults or fractures nearby
	Strength characteristics of surrounding rock	Uniaxial saturated compressive strength 90 MPa
	In situ stress coefficient	Ground stress coefficient 3
Structural defect	Lining thickness defect position	Arch waist
	Effective thickness ratio of lining	Effective thickness ratio 0.93
	Concrete strength	Concrete strength 0.95
	Defect site of lining steel bar	Arch waist
Structural stress	Lining pressure control	(Pressure zone) bending moment 35.6 kN·m (Pressure zone) Axial force 815.31 kN
	Lining tension control	(Tension zone) bending moment 42.14 kN·m (Tension zone) axial force 781.89 kN
Other factors	Construction design level	High level of construction design
	Seismic fortification intensity	Seismic fortification intensity 6
	Year of service	Three years

Detection of the above factors was brought into the membership function to obtain the relationship matrix, with R_1 representing the membership matrix of engineering geological conditions, R_2 the structural defect membership matrix, R_3 the surrounding rock (compression zone) membership matrix, R_4 the surrounding rock (tension zone) membership matrix, and R_5 the membership matrix of other factors. The details were as follows:

$$R_1 = \begin{pmatrix} 0.00 & 0.606 & 0.245 & 1.00 \\ 1.00 & 0.00 & 0.00 & 0.00 \\ 1.00 & 0.00 & 0.00 & 0.00 \\ 1.00 & 0.00 & 0.00 & 0.00 \\ 0.84 & 0.00 & 0.00 & 0.00 \\ 0.89 & 0.89 & 0.34 & 0.00 \end{pmatrix} \quad R_2 = \begin{pmatrix} 0.00 & 1.00 & 0.00 & 0.00 \\ 1.00 & 0.26 & 0.28 & 1.00 \\ 0.84 & 0.01 & 0.42 & 1.00 \\ 0.00 & 1.00 & 0.00 & 0.00 \end{pmatrix}$$

$$R_3 = \begin{pmatrix} 1.00 & 0.27 & 0.44 & 0.00 \\ 1.00 & 0.00 & 0.02 & 0.00 \end{pmatrix} \quad R_4 = \begin{pmatrix} 0.97 & 0.97 & 0.91 & 0.00 \\ 1.00 & 0.67 & 0.82 & 0.00 \end{pmatrix} \tag{22}$$

$$R_5 = \begin{pmatrix} 1.00 & 0.00 & 0.00 & 0.00 \\ 0.00 & 0.06 & 1.00 & 0.06 \\ 1.00 & 0.895 & 0.17 & 0.00 \end{pmatrix}$$

First-order fuzzy comprehensive evaluation was then conducted on the above relational matrix, with C_1 representing the fuzzy relational matrix of engineering geological conditions, C_2 the fuzzy relation matrix of structural defect factors, C_3 the fuzzy relation matrix of surrounding rock (compression zone), C_4 the fuzzy relation matrix of surrounding rock (tension zone), and C_5 the fuzzy relation matrix of other factors. The details were as follows:

$$\begin{aligned} C_1 &= a_1 \times R_1 = \begin{pmatrix} 1.035764 & 0.3351236 & 0.130057 & 0.1506 \end{pmatrix} \\ C_2 &= a_2 \times R_2 = \begin{pmatrix} 0.64589 & 0.49675 & 0.19353 & 0.65687 \end{pmatrix} \\ C_3 &= a_3 \times R_3 = \begin{pmatrix} 1.00 & 0.225 & 0.37 & 0.00 \end{pmatrix} \\ C_4 &= a_3 \times R_4 = \begin{pmatrix} 0.98 & 0.92 & 0.845 & 0.00 \end{pmatrix} \\ C_5 &= a_4 \times R_5 = \begin{pmatrix} 0.60 & 0.382 & 0.468 & 0.024 \end{pmatrix} \end{aligned} \tag{23}$$

The second-level fuzzy comprehensive evaluation was then carried out to obtain B_1, representing the final result of the second-level fuzzy comprehensive evaluation of the railway tunnel level III surrounding rock (compression zone) and B_2 the final result of the second-level fuzzy comprehensive evaluation of the railway tunnel level III surrounding rock (tension zone).

$$\begin{aligned} B_1 &= \begin{pmatrix} 0.857 & 0.3236 & 0.3221 & 0.17392 \end{pmatrix} \\ B_2 &= \begin{pmatrix} 0.85 & 0.689 & 0.569 & 0.174 \end{pmatrix} \end{aligned} \tag{24}$$

By processing the evaluation matrix with the principle of maximum membership degree, the safety level of the railway tunnel was obtained, for the level III surrounding rock monitoring section in tension zone and compression zones, the safety level was I. At this time, the tunnel was in a safe state, which was in line with the actual inspection of the engineering. Similarly, the health status of various surrounding rock levels of the railway tunnel was evaluated using fuzzy comprehensive evaluation. The results showed that the safety levels of the railway tunnel II and IV surrounding rock were at level I safety status and the safety level of the railway tunnel V surrounding rock at level II safety status.

The safety evaluation system can be applied to most railway tunnels. Through the analysis of different grades of surrounding rock structure, and the safety evaluation of Motianling, Xidashan and other typical railway tunnels. Due to the limited space, this paper only introduced the safety evaluation process of Motianling tunnel. The evaluation method can reflect the influence of various factors, and the evaluation conclusion is clear, accurate and practical, which is consistent with engineering practice. However, the fuzzy comprehensive algorithm also has limitations, and the determination of membership function and weight has certain subjectivity.

CONCLUSION

Safety evaluation of a railway-tunnel structure is a complex research subject. Establishing a practical comprehensive evaluation index system was of great significance for railway health detection. Based on the research and analysis of tunnel structural mechanics models, a safety assessment standard suitable for defect states was proposed here. A fuzzy comprehensive evaluation method was adopted for comprehensively evaluating the safety of railway-tunnel structures. The conclusions were summarized as:

(1) When assessing the railway tunnel, the safety factor was calculated according to the tensile control-bearing capacity of the vault in the range of a 60° central angle of the railway tunnel. At this time, the safety within the range of 60° central angle of the vault was shown to be of great importance for the tunnel design. Equations for the range of the central angle assessment were derived.

(2) Based on fuzzy comprehensive evaluation theory, a safety evaluation model of the railway tunnel structure was established. The membership function model of Gaussian distribution and ladder distribution were used to determine the membership grade of each impact factor and the weight of each factor determined by AHP. The multi-level fuzzy comprehensive evaluation method was used to evaluate the safety of an actual railway tunnel. The evaluation conclusions were examined using practical engineering. The evaluation algorithm comprehensively reflected the impact of various factors, was consistent with engineering practice, had strong practicality, and the evaluation conclusions clear and accurate.

ACKNOWLEDGEMENTS

This work was supported by the National Key R&D Program of China (Nos. 2018YFC0809600 and 2018YFC0809606), the Natural Science Foundation of Liaoning Province (No. 2019-MS-265), and Key Laboratory of the Ministry of Education on Safe Mining of Deep Metal Mines (No. 2019SMDM-KF-A01).

REFERENCES

[1] Li X.J., He F., Wang Y.B. et al., 2014. Tunnel Structure Safety Monitoring System Based on BOTDA Technology. Applied Mechanics and Materials, vol. 3368: 281-284.

[2] Ni X., Goodwine B., 2020. Damage modeling and detection for a tree network using fractional-order calculus. Nonlinear Dynamics, vol. 101: 875-891.

[3] Sun H., Liu S., Zhong R., Du L., 2020. Cross-Section Deformation Analysis and Visualization of Shield Tunnel Based on Mobile Tunnel Monitoring System. Sensors, vol. 20: 1006.

[4] Judit G., Joan R.C., Sergi V., 2020. Structural Health Monitoring with Distributed Optical Fiber Sensors of tunnel lining affected by nearby construction activity. Automation in Construction, vol. 117.

[5] Yang S., Zong L., Wang Y., 2011. Review on the research of highway bridges seismic damage assessment. Applied Mechanics and Materials, vol. 1446: 1224-1229.

[6] Hou G.Y., Xie B.B., Hu T., 2017. Fiber sheath effect in tunneling monitoring based on BOTDR technology. Rock and Soil Mechanics, vol. 38: 2441-2447.
[7] Lyu H., Shen S., Zhou A., 2022. Assessment of safety status of shield tunnelling using operational parameters with enhanced SPA. Tunnelling and Underground Space Technology incorporating Trenchless Technology Research, vol. 123.
[8] Fawad M., Koris K., Salamak M. et al., 2022. Nonlinear modelling of a bridge: A case study-based damage evaluation and proposal of Structural Health Monitoring (SHM) system. Archives of Civil Engineering, vol. 68: 569-584.
[9] Wierzbicki S., Pióro Z., Osiniak M., 2022. Laser-inclinometric method for displacement measurements in structural health monitoring. Archives of Civil Engineering, vol. 68: 607-616.
[10] Kazaras K., Kirytopoulos K., Rentizelas A., 2012. Introducing the STAMP method in road tunnel safety assessment. Safety Science, vol. 50: 1806-1817.
[11] Ou G., Jiao Y., Zhang G., 2021. Collapse risk assessment of deep-buried tunnel during construction and its application. Tunnelling and Underground Space Technology incorporating Trenchless Technology Research, vol. 115.
[12] Guo K., Zhang L., 2021. Multi-source information fusion for safety risk assessment in underground tunnels. Knowledge-Based Systems, vol. 227.
[13] Zhou S., Xiang Q., Wang Y., 2014. The Evaluation Method for Tunnel Structure Health Condition Based on Asymmetric Proximity. Applied Mechanics and Materials, vol. 2014: 1721-1727.
[14] Wang H., Noori M., Zhang J., 2016. A Wavelet-energy based damage identification method for steel bridges. Proceedings of the International Conference on Smart Infrastructure and Construction, vol. 2016.
[15] Pan Q., Dias D., 2017. Safety factor assessment of a tunnel face reinforced by horizontal dowels. Engineering Structures, vol. 142: 56-66.
[16] Alexakis H., Makris N., 2013. Minimum thickness of elliptical masonry arches. Acta Mechanica, vol. 224: 2977-2991.
[17] Yuan W., Guo A., Li H., 2017. Seismic failure mode of coastal bridge piers considering the effects of orrosion-induced damage. Soil Dynamics & Earthquake Engineering, vol. 93: 135-146.
[18] Liu X., Liu Y., Qu W., 2016. Internal force calculation and supporting parameters sensitivity analysis of side piles in the subway station excavated by Pile-Beam-Arch method. Tunnelling and Underground Space Technology incorporating Trenchless Technology Research, vol. 56: 186-201.
[19] Zhong C., Yang Q., Liang J., 2021. Fuzzy comprehensive evaluation with AHP and entropy methods and health risk assessment of groundwater in Yinchuan Basin, northwest China. Environmental Research, vol. 204: 111956-111956.
[20] Bai H., Wang N., 2010. Research on the selection of scale in AHP. IEEE, vol. 2010.
[21] Zul I., Indrani S., Adi A.J., 2022. Analysing dimensions and indicators to design energy education framework in Malaysia using the analytic hierarchy process (AHP). Energy Reports, vol. 8: 1013-1024.
[22] Hamidah M., Hasmadi I., 2022. Development of a protocol for Malaysian Important Plant Areas criterion weights using Multi-criteria Decision Making-Analytical Hierarchy Process (MCDM-AHP). Global Ecology and Conservation, vol. 34: e02033.
[23] Li T., Yang B., 2010. Study on green logistics operation system of port based on AHP-fuzzy comprehensive evaluation. IEEE, vol. 2010.
[24] Zhang J.W., Wang S., Huang H.X., 2014. Study on Classification and Regulation for Defects on Railway Tunnel. Applied Mechanics and Materials, vol. 3307: 1207-1211.
[25] Wang Q., Yang J., Liang Y., 2020. Prediction of time-dependent behaviour of steel–recycled aggregate concrete (RAC) composite slabs via thermo-mechanical finite element modelling. Journal of Building Engineering, vol. 29: 101191.